

# The next-generation sphingosine-1 receptor modulator BAF312 (siponimod) improves cortical network functionality in focal autoimmune encephalomyelitis

Petra Hünedehege<sup>1,\*,#</sup>, Manuela Cerina<sup>1,#</sup>, Susann Eichler<sup>1,#</sup>, Christian Thomas<sup>1</sup>, Alexander M. Herrmann<sup>1</sup>, Kerstin Göbel<sup>1</sup>, Thomas Müntefering<sup>1</sup>, Juncal Fernandez-Orth<sup>1</sup>, Stefanie Bock<sup>1</sup>, Venu Narayanan<sup>1</sup>, Thomas Budde<sup>2</sup>, Erwin-Josef Speckmann<sup>2</sup>, Heinz Wiendl<sup>1</sup>, Anna Schubart<sup>3</sup>, Tobias Ruck<sup>1</sup>, Sven G. Meuth<sup>1</sup>

1 Department of Neurology with Institute of Translational Neurology, Westfälische Wilhelms-Universität, Münster, Germany

2 Institute of Physiology I, Westfälische Wilhelms-Universität, Münster, Germany

3 Novartis Institutes of Biomedical Research, Basel, Switzerland

**Funding:** This study was supported by the Novartis Institutes of Biomedical Research, Basel, Switzerland (to SGM).

## Abstract

Autoimmune diseases of the central nervous system (CNS) like multiple sclerosis (MS) are characterized by inflammation and demyelinated lesions in white and grey matter regions. While inflammation is present at all stages of MS, it is more pronounced in the relapsing forms of the disease, whereas progressive MS (PMS) shows significant neuroaxonal damage and grey and white matter atrophy. Hence, disease-modifying treatments beneficial in patients with relapsing MS have limited success in PMS. BAF312 (siponimod) is a novel sphingosine-1-phosphate receptor modulator shown to delay progression in PMS. Besides reducing inflammation by sequestering lymphocytes in lymphoid tissues, BAF312 crosses the blood-brain barrier and binds its receptors on neurons, astrocytes and oligodendrocytes. To evaluate potential direct neuroprotective effects, BAF312 was systemically or locally administered in the CNS of experimental autoimmune encephalomyelitis mice with distinct grey- and white-matter lesions (focal experimental autoimmune encephalomyelitis using an osmotic mini-pump). *Ex-vivo* flow cytometry revealed that systemic but not local BAF312 administration lowered immune cell infiltration in animals with both grey and white matter lesions. *Ex-vivo* voltage-sensitive dye imaging of acute brain slices revealed an altered spatio-temporal pattern of activation in the lesioned cortex compared to controls in response to electrical stimulation of incoming white-matter fiber tracts. Here, BAF312 administration showed partial restore of cortical neuronal circuit function. The data suggest that BAF312 exerts a neuroprotective effect after crossing the blood-brain barrier independently of peripheral effects on immune cells. Experiments were carried out in accordance with German and EU animal protection law and approved by local authorities (Landesamt für Natur, Umwelt und Verbraucherschutz Nordrhein-Westfalen; 87-51.04.2010.A331) on December 28, 2010.

**Key Words:** multiple sclerosis; focal experimental autoimmune encephalomyelitis; cortical grey matter; white matter; BAF312; neuroaxonal damage; neuroprotection

**Chinese Library Classification No.** R453; R363; R741

## Introduction

Multiple sclerosis (MS) is an autoimmune central nervous system (CNS) disease characterized by demyelination and neurodegeneration. The most common disease course (relapsing MS, RMS), affects approximately 85% of patients and manifests with recurring focal neurological deficits followed by total or partial recovery. Progressive forms of MS (PMS) are defined by the accumulation of neurological disability occurring independently of relapses (Lublin et al., 2014). Focal demyelinated lesions with variable degrees of inflammation (Kuhlmann et al., 2017) are found in white matter regions, cerebral cortex (Kidd et al., 1999; Bø et al., 2003b) and in deep brain structures like the thalamus (Deppe et al., 2016). While cortical damage and grey matter lesions can already be found in early stages of the disease (Haider et al., 2014; Mandolesi, 2015), cortical demyelination is the most pronounced hallmark in PMS (Haider et al., 2014). In patients with RMS, MS lesions contain a high number of

macrophages, microglia and perivascular T cells (Kuhlmann et al., 2017). In contrast, lesions of patients with PMS, are mainly characterized by neuroaxonal damage and a small number of inflammatory cells (Frischer et al., 2015). In line with these findings, disease-modifying treatments altering or suppressing the immune system were beneficial in RMS patients, but most of these drugs failed to ameliorate disability progression in PMS (Montalban et al., 2017). Hence, suitable drugs that promote the latter process are urgently needed.

Siponimod (BAF312), a novel sphingosine-1 receptor (S1P-R) modulator selectively targeting S1P1-R and S1P5-R (Pan et al., 2013), showed to ameliorate disability progression in patients with PMS, including ones who reached a non-relapsing stage in one recent large clinical trial (EXPAND (Kappos et al., 2018)). Mechanistically, beside reducing inflammation by sequestering lymphocytes in lymphoid tissues, BAF312 crosses the blood-brain barrier and binds its receptors on neurons, astrocytes and oligodendrocytes influ-

## \*Correspondence to:

Petra Hünedehege, PhD,  
petra.huedehege@ukmuenster.de.

#These authors contributed  
equally to this work.

## orcid:

0000-0001-9562-0285  
(Petra Hünedehege)

doi: 10.4103/1673-5374.259622

Received: February 9, 2019

Accepted: May 7, 2019

encing regulation of astrogliosis (Choi et al., 2011), modulating oligodendrocyte processes and cell survival (Jaillard et al., 2005). Recently, evidence of a potential neuroprotective effect of BAF312 administration were shown in an animal model of experimental autoimmune encephalomyelitis (EAE) with beneficial effect on clinical scores, significant reduction of astro-microgliosis and improvement of GABAergic transmission in the striatum (Gentile et al., 2016).

However, while EAE is the most frequently used active immunization model in which animals are immunized with the myelin oligodendrocyte glycoprotein 35–55 (MOG<sub>35–55</sub>) peptide (Mendel et al., 1995; Bittner et al., 2014), inflammatory lesions are typically confined to the spinal cord and occur in the brain in randomly distributed locations (Pomeroy et al., 2005; Storch et al., 2006). However, studying neurodegenerative aspects in a reproducible localization of brain lesions is achieved by performing focal grey matter lesions induced in MOG<sub>35–55</sub> immunized mice through injection of interferon- $\gamma$  (IFN- $\gamma$ ) and tumor necrosis factor  $\alpha$  (TNF- $\alpha$ ), thus allowing the study of cortical lesion pathophysiology and treatment effects (Chaudhary et al., 2015; Lagumersindez-Denis et al., 2017).

This study aimed to dissect the peripheral immunomodulatory effects of BAF312 from potential direct neuroprotective effects in the CNS. For this purpose, we took advantage of a multidimensional approach by using a focal EAE model with distinct grey or white matter lesions and administering BAF312 either systemically or intracerebrally using osmotic mini-pumps. The effects of BAF312 on the inflammatory response in focal cortical grey and white matter lesions were analyzed by using multicolor flow cytometry. In addition, the integrity of the thalamocortical neuronal network circuits was assessed using a voltage sensitive dye technique.

## Material and Methods

### Focal EAE Model

Experiments were carried out in accordance with German and EU animal protection law and approved by local authorities (Landesamt für Natur, Umwelt und Verbraucherschutz Nordrhein-Westfalen; 87-51.04.2010.A331) on December 28, 2010. EAE was induced as described previously (Bittner et al., 2014; Göbel et al., 2016b). Briefly, 10 days prior to focal EAE induction, C57BL/6J mice (female, ~10 weeks, Envigo, Rossford, Germany) were subcutaneously immunized with 200  $\mu$ g of murine MOG<sub>35–55</sub> peptide (Charité, Berlin, Germany) emulsified in 200  $\mu$ L complete Freund's adjuvant (Merck KGaA, Darmstadt, Germany; former name Sigma-Aldrich Chemie GmbH, Steinheim, Germany) containing 200  $\mu$ g Mycobacterium tuberculosis (strain H37 Ra; Becton, Dickinson and Company (BD), Sparks, MD, USA). Pertussis toxin (400 ng in 200  $\mu$ L phosphate-buffered saline (PBS); Enzo Life Sciences, Farmingdale, NY, USA) was injected intraperitoneally (i.p.) on the day of immunization (day 0) and 2 days later. The clinical course of EAE was monitored daily by two blinded investigators using the following scoring system: grade 0, no abnormality; grade 1, limp tail tip; grade 2, limp tail; grade 3, moderate hindlimb weakness; grade 4, com-

plete hindlimb weakness; grade 5, mild paraparesis; grade 6, paraparesis; grade 7, heavy paraparesis or paraplegia; grade 8, tetraparesis; grade 9, quadriplegia or premoribund state; or grade 10, death. Animals with a score of 8 were killed and the last score observed was included in the analysis until the end of the experiment. Ten days after MOG immunization (10 d.p.i.), mice were anesthetized and mounted on a stereotaxic device. A hole was drilled through the skull using the following coordinates: anteroposterior, -2.18 mm; lateral, 4.2 mm from bregma; and dorsoventral, 1 mm from the brain surface for the auditory cortex (AC), and anteroposterior, -0.94 mm; lateral, 2.10 mm; dorsoventral, 2.5 mm for the internal capsule (IC) (Paxinos and Franklin, 2001). Two  $\mu$ L of pro-inflammatory cytokine solution containing TNF- $\alpha$  (150 U; Merck KGaA) and 800 U of IFN- $\gamma$  (Merck KGaA) dissolved in PBS was slowly injected either into AC or the IC of the left hemisphere. The contralateral hemisphere (right side) was used as control. Mice were sacrificed 2 days post injection (day 12; **Figure 1a** and **d**). An additional group of mice used for histopathological evaluation only was sacrificed 5 days post-injection (**Figure 3**).

### Oral and intracerebral BAF312 treatment

For systemic application, BAF312 (3 mg/kg; Novartis Pharma AG, Basel, Switzerland) was administered daily *via* oral gavage in 1% aqueous carboxy-methylcellulose. For intracerebral application, BAF312 was dissolved in a solution containing 10% Solutol/Kolliphor HS15 (BASF Pharma Solutions, Ludwigshafen am Rhein, Germany) with a final pH range between 6 and 7 at a final concentration of 2 mg/mL. This preparation allowed stability of the drug for up to 6 weeks at 37°C. At the day of focal EAE induction, mice were implanted with subcutaneous osmotic mini pumps (Alzet Osmotic Pumps, Cupertino, CA, USA) allowing continuous intracerebral (i.c.) infusion of either vehicle or BAF312 (0.3 and 1  $\mu$ g/d) to the focal lesion site.

### Flow cytometry

Multicolor flow cytometric analyses of murine peripheral leukocytes were performed as previously described (Göbel et al., 2016a). Prior to staining, EDTA-blood was treated with red blood cell (RBC) lysis buffer according to the manufacturer's protocol (BioLegend, London, UK). For purification of brain-infiltrating leukocytes, brains from animals were removed after transcardial perfusion with PBS in order to efficiently remove circulating blood. Brain slices of lesioned *vs.* non-lesioned hemispheres were prepared and mechanically homogenized in PBS, layered on a 30–50% Percoll (Merck KGaA) gradient and continuously centrifuged for 30 minutes at around 1300  $\times$  g. Mononuclear cells were isolated at the interphase. After isolation, leukocytes were stained for 30 minutes at 4°C with the appropriate combination of indicated fluorescence-labeled monoclonal antibodies in PBS containing 0.1% NaN<sub>3</sub> (Merck KGaA) and 0.1% bovine serum albumin (BSA) (Merck KGaA). Corresponding isotype controls were used for the staining. For blocking of Fc receptors, cells were preincubated with purified anti-CD16/CD32

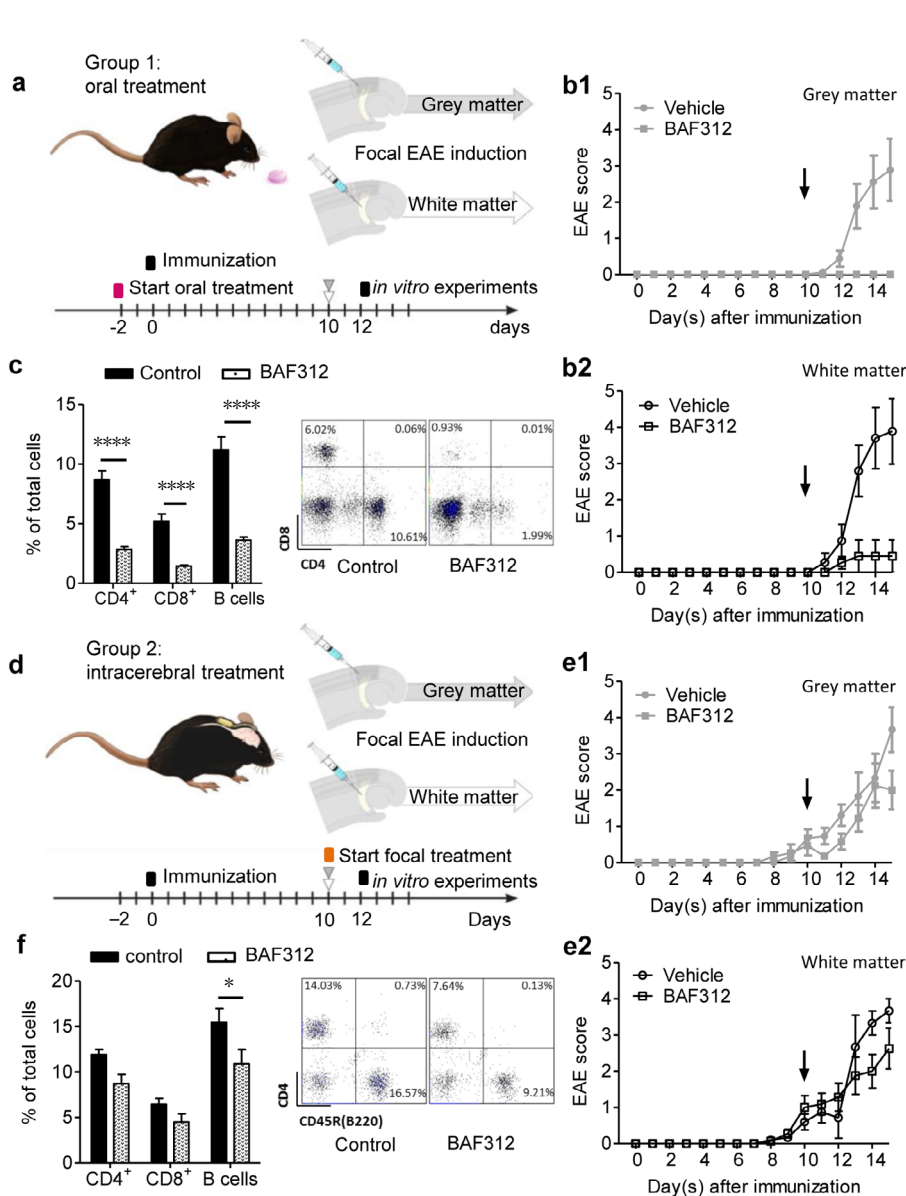


**Figure 1** Oral, but not intracerebral treatment with BAF312 ameliorates the disease course in the focal EAE model with grey and white matter lesions.

(a, d) Experimental scheme. 10 days after immunization (day 0) with MOG<sub>35-55</sub> peptide in C57BL/6J mice, focal EAE lesions were induced by stereotactical injection of proinflammatory cytokines (interferon- $\gamma$  and tumor necrosis factor  $\alpha$ ) into the auditory cortex or the internal capsule to induce cortical grey or white matter lesions, respectively. There were two experimental groups: Group 1 received BAF312 (a sphingosine-1-phosphate receptor modulator) *via* oral gavage (3 mg/kg) versus vehicle starting 2 days before immunization, and group 2 received continuous intracerebral injection of BAF312 (1  $\mu$ g/d) versus vehicle using an osmotic mini pump from the day of focal EAE induction. (b) Clinical courses of focal EAE mice with cortical grey matter lesions (b1) or white matter lesions (b2) that received oral BAF312 application (3 mg/kg). The vertical black arrows indicate the time point corresponding to induction of focal EAE (10 days post induction). (c) Bar graph showing the percentage of peripheral blood lymphocyte counts two days after focal EAE induction (upper panel). The panel below shows a representative scatter plot for CD4<sup>+</sup> and CD8<sup>+</sup> T lymphocytes. (e) Clinical courses of focal EAE mice with cortical grey matter lesions (e1) or the white matter lesion group (e2) that received continuous intracerebral injection of BAF312 (1  $\mu$ g/d). (f) Bar graph showing the percentage of peripheral blood lymphocytes two days after pump implantation. The panel below shows a representative scatter plot for CD4<sup>+</sup> and B (CD45R(B220)<sup>+</sup>) lymphocytes. \* $P < 0.05$  and \*\*\* $P < 0.0001$  (two-way analysis of variance with Bonferroni *post-hoc* test). The right panel shows a representative scatter plot for CD4<sup>+</sup> and CD45R(B220) lymphocytes. EAE: Experimental autoimmune encephalomyelitis; Siponimod (BAF312): novel sphingosine-1 receptor modulator.

antibody (BioLegend, 1.0  $\mu$ g per  $10^6$  cells in 100  $\mu$ L volume) for 5 minutes on ice prior to immunostaining. The following mAbs were used for the detection of cell surface markers: CD3 (clone 17A2, BioLegend), CD4 (clone RM4-5, BioLegend), CD8a (clone 53-6.7, BioLegend), CD11b (clone M1/70, eBioscience), CD45 (clone 30-F11, BioLegend) and CD45R (also known as B220; clone RA3-6B2, BD). Concentrations of mAbs were carefully titrated prior to experiments. Stained cells were assayed on a Gallios flow cytometer (Beckman Coulter, Krefeld, Germany) using Kaluza software (Beckman Coulter).

### Immunofluorescence staining

In order to verify the injection site, evaluate myeloid cells infiltration from the periphery and neuronal survival brains were used for histopathological evaluation. Briefly, mice were deeply anesthetized using ketamine/xylazine and transcardially perfused using phosphate-buffered saline (PBS),

in order to efficiently remove circulating blood, as described before (Cerina et al., 2017). Afterwards, brains were quickly removed, embedded in cryoprotective compound (TissuTeK, Science Service GmbH, Munich, Germany) and frozen using liquid nitrogen. Coronal cryo-sections (10  $\mu$ m thickness) were cut using a cryotome (Leica, Wetzlar, Germany), positioned on glass slides (two per slide) and conserved at  $-20^{\circ}\text{C}$ . Slices were fixed in a solution containing 4% paraformaldehyde (PFA) for 10 minutes and then washed with PBS. In order to avoid false-positive results, slices were incubated overnight at  $4^{\circ}\text{C}$  with a blocking solution containing PBS, 0.03% Triton X-100, 10% goat serum and 10% BSA. After blocking, slices were incubated with the primary antibody CD11b to identify myeloid cells (1:200, rat anti mouse; Bio-Rad Laboratories GmbH, Hercules, CA, USA; former name Serotec, Puchheim, Germany). The antibody was diluted in a cold solution containing 1% donkey serum, 10% BSA and PBS. Overnight incubation followed. Slides were then

incubated for 1 hour with fluorophore-conjugated secondary antibody: Cyanine Cy3 (1:300, donkey anti-rat; Jackson ImmunoResearch Inc., Cambridgeshire, UK). Finally, the mounting medium Fluoromount-G containing DAPI (Thermo Fisher Scientific, Darmstadt, Germany; former name Invitrogen, San Diego, CA, USA) was applied as marker for cell nuclei. For evaluating apoptosis, we performed TUNEL/NeuN staining using an *in situ* cell death detection kit with fluorescein according to manufacturer's instructions (In Situ Cell Death Detection Kit with Fluorescein, Roche *via* Merck KGaA).

### Immunohistochemistry analysis

Images were acquired using a Zeiss Examiner microscope (Zeiss, Göttingen, Germany). Images of slices containing the AC were collected from both hemispheres. All image analyses were performed in a blinded manner using ImageJ (open source image processing software (<https://imagej.nih.gov/ij/index.html>); Schneider et al., 2012). Images were acquired using 10- and 20-fold objectives and analyzed by counting the number of CD11b<sup>+</sup> cells per mm<sup>2</sup>. For TUNEL/NeuN images were acquired using a 20-fold objective and analyzed by counting the number of fluorescence positive cells per mm<sup>2</sup>.

### Voltage-sensitive dye technique and analysis

EAE and focal EAE were induced as described above. Two days after cytokine injection for inducing focal EAE, the animals were deeply anesthetized and the brains quickly removed. Brains were glued onto an agar block with a 25° angle in order to cut (vibratome from Leica) sagittal slices (500 µm of thickness) containing the full-functioning auditory thalamocortical (TC) system (Broicher et al., 2010; Ghaffarian et al., 2016). Cutting was performed in ice-cold artificial-cerebrospinal fluid (ACSF) solution containing the following in mM: sucrose, 200; glucose, 10; PIPES, 20; KCl, 2.5; MgSO<sub>4</sub>, 10; CaCl<sub>2</sub>, 0.5; pH 7.35 with NaOH. Slices were then incubated with the voltage-sensitive dye RH-795 (12 µg/mL, Thermo Fisher Scientific, Waltham, MA, USA) in oxygenated ACSF for 60 minutes at 30°C. Afterwards, slices were transferred to an incubation chamber and experiments started after 60 minutes, the time necessary to wash-out the additional dye. Optical signal recordings were performed at 30°C in carbonated ACSF in a submerged chamber on an inverted microscope (Zeiss, Göttingen, Germany). Every slice was tested twice: in the absence (as control) and in the presence of BAF312 (10 µM). Optical recordings were performed in the primary AC as described previously (Broicher et al., 2010) and governed by the software Neuroplex (Redshirt Imaging, Decatur, GA, USA). Fluorescence changes were detected using a hexagonal photodiode array consisting of 464 elements through a 20× objective covering the whole AC in a given slice (Figure 4a). The sampling interval was 1.274 ms and the maximal length of the recording was 1.305 ms. The excitation wavelength of RH-795 was bandpass filtered at 546 ± 20 nm, and after passing a dichroic mirror, emitted light was highpass filtered at 590 nm with transmission and emission maxima being 530 and 712 nm, respectively. Opti-

cal signals were detected as fractional changes of the fluorescence from the resting light intensity ( $(I_{rest} - I_{recording})/I_{rest}$ ; dI/I in the text). Color-coded activity maps were constructed using the spatiotemporal cortical inputs recorded as fluorescence signals. Scales were calculated for each recording based on the maximal calculated amplitude and therefore are different in every experimental condition.

### Statistical analysis

For each type of experiment, group sizes are given in the figure legends. Statistical analyses and graphs were prepared using Prism 5.04 (Graph Pad, San Diego, CA, USA). Data were presented as the mean ± SEM. The significance level was set to  $P < 0.05$ . Statistical analysis was performed using Student's *t*-test for comparisons between groups and non-parametric Mann-Whitney *U* test, where needed. Multiple comparisons were analyzed by Kruskal-Wallis test followed by Dunn's *post-hoc* test and by two-way analysis of variance (ANOVA) with Bonferroni *post-hoc* test for independent measures.

## Results

### Oral, but not intracerebral treatment with BAF312 ameliorates the disease course in a focal EAE mouse model with grey and white matter lesions

To investigate effects of BAF312 treatment on cortical grey and subcortical white matter inflammatory lesions in a focal EAE model, C57BL/6J mice were immunized with MOG<sub>35-55</sub> peptide 10 days prior to stereotactical injection of proinflammatory cytokines (IFN-γ and TNF-α) in either the AC or the internal capsule (IC) to induce cortical grey or white matter lesions, respectively (day 0; Figure 1a and d). Furthermore, we differentiated between oral administration of BAF312 from 2 days prior to immunization (group 1, AC: vehicle [ $n = 19$ ], BAF312 [ $n = 20$ ] and IC: vehicle [ $n = 17$ ], BAF312 [ $n = 22$ ]; Figure 1a) and direct delivery of the drug into the brain using an osmotic mini pump with continuous intracerebral infusion starting at the day of focal EAE induction (10 d.p.i.; group 2, AC: vehicle and BAF312 [ $n = 30$ ] and IC: vehicle [ $n = 30$ ] and BAF312 [ $n = 29$ ]; Figure 1d).

Independent of the induced lesion site, the effect of systemic BAF312 treatment (3 mg/kg) led to significantly reduced disease severity throughout the whole observation period of 15 days compared to the vehicle-treated group (Figure 1b). In line with the previous report (Gergely et al., 2012), animals orally treated with BAF312 showed only minimal clinical symptoms during the whole observation period. As expected, flow cytometry analysis of peripheral blood indicated a significant lymphopenia of orally treated mice ( $n = 23$ ) compared to those treated with vehicle ( $n = 23$ ; open and black bars, respectively; CD4<sup>+</sup> T lymphocytes:  $2.83 \pm 0.25\%$  vs.  $8.70 \pm 0.72\%$ , respectively; CD8<sup>+</sup> T lymphocytes:  $1.44 \pm 0.09\%$  vs.  $5.20 \pm 0.62\%$ , respectively; B cells:  $3.61 \pm 0.27\%$  vs.  $11.19 \pm 1.07\%$ , respectively; two-way ANOVA,  $F_{(2,132)} = 133.9$ ;  $P < 0.0001$ , Bonferroni *post-hoc* test: all controls vs. BAF312-treated groups,  $P < 0.001$ ; Figure 1c). To distinguish between systemic and direct effects on the brain, we performed local administration of BAF312 using an osmotic

minipump (**Figure 1d**). Given that in the literature the intra-cerebroventricular application of 0.45  $\mu\text{g/d}$  was reported to induce lymphopenia (Gentile et al., 2016), we performed a dose-response screening using a higher and lower concentration of BAF312, namely 1  $\mu\text{g/d}$  and 0.3  $\mu\text{g/d}$ , respectively, *via* intracerebral application in order to target only confined brain regions and evaluate if local treatment will induce peripheral effects (**Additional Figure 1**). The effects induced by application of both concentrations did not differ concerning the total number of CD4<sup>+</sup> T lymphocytes, CD8<sup>+</sup> T lymphocytes and B cells obtained from peripheral blood (control  $n = 4$ , 0.3  $\mu\text{g/d}$  BAF312,  $n = 4$ ; **Additional Figure 1a**) and lymph nodes (**Additional Figure 1b**). Therefore, we assume that any biological effect after intracerebral treatment is central and decided to use the BAF312 concentration of 1  $\mu\text{g/d}$  for all the following experiments. On a clinical level, intracerebral application of 1  $\mu\text{g/d}$  BAF312 did not affect the motor disability of EAE mice throughout the observation period of 15 days compared to non-treated controls (**Figure 1e**). This was irrespective of the lesion site (grey matter *vs.* white matter) and, therefore, region of drug infusion. Unlike in the orally treated animals, two days after starting continuous intracerebral administration of BAF312 ( $n = 14$ ), we could not detect a decrease of the total number of CD4<sup>+</sup> and CD8<sup>+</sup> T lymphocytes in the peripheral blood in comparison to controls ( $n = 19$ ; CD4<sup>+</sup> lymphocytes:  $8.70 \pm 1.02\%$  *vs.*  $11.90 \pm 0.57\%$ , respectively; CD8<sup>+</sup> lymphocytes:  $4.50 \pm 0.91\%$  *vs.*  $6.44 \pm 0.64\%$ , respectively; **Figure 1f**). However, a small but significant difference between BAF312- and vehicle-treated mice was observed by evaluating the percentage of B cells ( $10.89 \pm 1.56\%$  *vs.*  $15.47 \pm 1.52\%$ , respectively; two-way ANOVA,  $F_{(2,93)} = 12.85$ ,  $P = 0.0005$ ; Bonferroni *post-hoc* test: control *vs.* BAF312-treated group,  $P < 0.05$ ; **Figure 1f**).

#### **Intracerebral BAF312 treatment does not reduce harmful immune cell infiltration into the brain parenchyma compared to non-treated controls**

As active EAE lesions are characterized by hypercellularity and prominent infiltration of T lymphocytes, we next examined the composition of immune cells as assessed by *ex vivo* brain slices that were retrieved two days after focal lesion induction. The slices were split into the lesioned and the non-lesioned hemisphere and subsequently analyzed by multicolor flow cytometry. In mice with focal EAE orally treated with BAF312, total leukocyte counts (CD45<sup>+</sup> cells) were increased on the lesioned hemisphere compared to the contralateral hemisphere (two way ANOVA, effect of the lesion site:  $F_{(1,16)} = 27.52$ ,  $P < 0.0001$ ) independent of a grey or white matter lesion (**Figure 2a**). Oral BAF312 (B) treatment (**Figure 2b**) resulted in a notably lower number of leukocytes within the lesioned hemisphere compared to vehicle-injected (V) controls (AC lesioned, V:  $1 \pm 0.22$  *vs.* B:  $0.40 \pm 0.14$  and IC lesioned: V:  $1.22 \pm 0.21$  *vs.* B:  $0.22 \pm 0.03$ ; two-way ANOVA, effect of BAF312 treatment:  $F_{(3,16)} = 10.44$ ,  $P = 0.001$ ; Bonferroni *post-hoc* test in lesioned hemisphere: grey-matter control *vs.* grey-matter BAF312,  $P < 0.05$  and white-matter control *vs.* white-matter BAF312,  $P < 0.001$ ; **Figure 2a**).

Analyzing lymphocyte subpopulations, CD4<sup>+</sup> T lymphocyte infiltration was found to be reduced in both the cortical grey matter (V:  $1 \pm 0.18$  *vs.* B:  $0.09 \pm 0.07$ , Student's *t*-test:  $t = 4.64$ ,  $df = 4$ ,  $P = 0.009$ ; **Figure 2b**) and subcortical white matter lesioned hemisphere of orally treated animals in comparison to vehicle-treated animals (V:  $1 \pm 0.22$  *vs.* B:  $0.04 \pm 0.007$ , Student's *t*-test:  $t = 4.31$ ,  $df = 4$ ,  $P = 0.012$ ; **Figure 2b**). Counts of CD8<sup>+</sup> T lymphocytes were found to be nominally and significantly lower in cortical grey and white matter lesions, respectively (white matter lesion, Student's *t*-test:  $t = 8.02$ ,  $df = 4$ ,  $P = 0.0013$ ; **Figure 2c**). In comparison, continuous intracerebral application of BAF312 through an osmotic mini pump neither resulted in any notable changes of total CD45<sup>+</sup> leukocytes (two-way ANOVA, effect of BAF312 treatment,  $F_{(3,30)} = 1.46$ ,  $P = 0.24$ ; **Figure 2d**) nor CD4<sup>+</sup> (grey matter,  $P = 0.99$ , and white matter:  $P = 0.11$ ; **Figure 2e**) or CD8<sup>+</sup> lymphocyte counts in the lesioned hemispheres (grey matter,  $P = 0.06$  and white matter:  $P = 0.18$ ; **Figure 2f**).

These results were corroborated by immunofluorescence staining performed to identify infiltrating peripheral myeloid cells, including macrophages in the AC. Counting the cells revealed a tendency to decreased number of CD11b<sup>+</sup> cells 2 days after cytokine injection in orally treated mice in comparison to the ones that received vehicle ( $253.7 \pm 63.3$  cells/mm<sup>2</sup> and  $743.3 \pm 125.7$  cells/mm<sup>2</sup>, respectively, **Figure 3a**). In the immunofluorescence analysis, the values reached significance threshold 5 days after focal cytokine injection when the oral treatment with BAF312 decreased the number of CD11b<sup>+</sup> cells/mm<sup>2</sup> from  $4197 \pm 778$  to  $326 \pm 61$  (Kruskal-Wallis test: 10.60,  $P = 0.0141$ , Dunn's *post-hoc* test:  $P = 0.0204$ ; **Figure 3a**). Local application of BAF312 showed a similar trend but values did not reach significance threshold at any of the analyzed time points (**Figure 3a**). Further analysis to assess neuroprotective effects of intracerebral administration of BAF312 was performed by investigating the effects of the drug on neuronal apoptosis. Immunofluorescence staining with the specific marker TUNEL/NeuN showed a tendency to a reduced apoptosis in the BAF312-treated group 2 days after focal cytokine injection (**Figure 3b**).

#### **BAF312 positively affects increased neuronal network activity in the AC of a focal EAE mouse model**

Next, we sought to assess the effect of BAF312 administration at the neuronal network level in the primary AC. We therefore prepared acute brain slices containing AC and IC obtained from MOG<sub>35-55</sub> immunized mice two days after cytokine injections, and incubated them with a voltage sensitive-dye. Changes in cortical neuronal activity, evoked by electrical stimulation in the IC, could be detected as fractional changes of fluorescence signals. The usage of a photodiode array (red hexagonal structure in **Figure 4a**) ensured detection of the fluorescence changes in a very precise spatio-temporal manner. The latter consists of 464 small photo-diodes which anatomically overlap with AC, thereby allowing analysis of the activity of the different layers of the cortex over a time period of 1.3 seconds. Taken together, the

information provided by all diodes can be used to construct color-coded fluorescence maps of AC neuronal network activity. Our maps showed a physiological activation of AC following electrical stimulation (stim) in naïve animals. In more detail, incoming stimuli quickly propagate to the upper part of AC which in the hexagonal maps corresponds to its upper-red colored part (first map from the left, 5.0–10 ms, **Figure 4b**). Afterwards, the stimuli propagate to lower parts of the cortex (39.5–44.5 ms, **Figure 4d**), where populations of neurons generating connections to subcortical regions further processes and discriminate information (Barbour and Callaway, 2008; Broicher et al., 2010). Interestingly, our approach revealed how a focal inflammatory lesion in AC changed this pattern of activity by affecting the spatio-temporal propagation of the stimulus (second map from the left, **Figure 4b**). The same electrical stimulation evoked an extensive response in control animals with focal EAE: the entire AC was activated (as indicated by the deep-red colored map, white arrows in the second map from the left, **Figure 4b**). Moreover, while the response decreases between 7.5 and 10 ms after stimulation in the naïve animals, cortical activation persists in animals with focal EAE indicating an altered propagation and spatial distribution of the stimuli. Adding BAF312 (10  $\mu$ M, (O'Sullivan et al., 2016)) to the bath improved this condition by reducing the persistent activation observed in control animals with focal EAE, as indicated by the white arrows in the third map from the left starting at 7.5 ms after stimulation. Exemplary fluorescence signals (**Figure 4c**) were recorded in the area contained in the black circle in the second and third map from the left, **Figure 4b**). They show a reduced amplitude of the response in BAF312 treated slices in comparison to the slices obtained from control animals with focal EAE indicating an improved propagation of the stimulus. Of note, besides decreasing the amplitude of the response, application of BAF312 induced a sharp repolarization after neuronal activation, indicated by the black arrow in the exemplary fluorescence signals of **Figure 4c**, which was not observed in slices obtained from animals with focal EAE.

Analyzing later time points after stimulation (39.5–44.5 ms, **Figure 4d**) in order to investigate the propagation to lower layers of the cortex showed a lack of the latter in slices obtained from control animals with focal EAE. The lower part of the fluorescence map (second from the left, **Figure 4d**) show a preponderance of green colors in comparison to the red-color coded region of naïve animals (first map from the left, **Figure 4d**). Adding BAF312 to the bath increased the stimulus propagation after 42 ms from the stimulation as indicated by the white arrows in the third map from the left. Moreover, exemplary signals recorded from the same area investigated at early time points after stimulation (indicated by the black circle in **Figure 4d**), also showed a slight increase in the amplitude, corroborating the findings (**Figure 4e**).

## Discussion

MS is a prototypical autoimmune inflammatory disease of the CNS and challenges both researchers and physicians due

to the coexistence of inflammatory and neurodegenerative disease mechanisms. While current treatment approaches almost exclusively focus on the immune pathology, neurodegenerative aspects are not sufficiently acknowledged (Klotz et al., 2019). This is partly owed to the fact that pathophysiological aspects of neurodegeneration are not sufficiently recapitulated and analyzed in the most commonly used model, EAE (Toader et al., 2018). Here, pre-immunization with MOG<sub>35–55</sub> peptide leads to disseminated and variable inflammatory CNS lesions with a predilection of the spinal cord (Johns et al., 1995; Lassmann and Bradl, 2016). By virtue of these characteristics, a correlation of functional and structural deficits is very complex and often impossible. This holds true especially for studying cortical lesions that represent a hallmark of primary and secondary PMS and are considered to be strongly involved in the process of neurodegeneration (Haider et al., 2014).

In the present study, we investigated the effects of BAF312 in preventing autoimmune neurodegeneration and took advantage of a modified EAE model with targeted induction of cortical grey matter and subcortical white matter lesions. In the past years, several attempts have been made to develop a localized model for MS that resembles histopathological features of human MS. Proinflammatory cytokines have been widely used to study CNS inflammation (Simmons and Willenborg, 1990; Sun et al., 2004). Local administration of IFN- $\gamma$  and TNF- $\alpha$  either by stereotactical injection into the spinal cord (Kerschensteiner et al., 2004) and brain of Lewis rats (Merkler et al., 2006) and C57BL/6 mice (Chaudhary et al., 2015; Lagumersindez-Denis et al., 2017), or by adenovirus transfection (Silva et al., 2018) resulted in cortical grey matter, subcortical and spinal white matter demyelination sharing striking similarity with human MS. While cortical lesions showed only transient inflammatory infiltration (Merkler et al., 2006; Chaudhary et al., 2015), white matter lesions in the spinal cord and in the corpus callosum displayed persistent infiltration with macrophages and microglia (Kerschensteiner et al., 2004; Merkler et al., 2006), suggesting that this model allows to recapitulate different types of autoimmune pathology depending on the site of lesion induction. Here, we adopted this experimental approach to target white and grey matter regions within the same extended network, namely the internal capsule or the AC. Both are known to be well-organized structures within the TC system, thereby making functional analysis possible (Broicher et al., 2010; Cerina et al., 2017). Moreover, we decided to use this relatively new model to test a potential neuroprotective effect of BAF312.

BAF312 is a S1P receptor modulator that crosses the blood-brain barrier and targets different receptor subtypes that have been shown to be involved in T cell migration into the CNS, astrogliosis, oligodendrocyte process modulation and cell survival (Bigaud et al., 2014; O'Sullivan et al., 2016). Therefore, BAF312 is an interesting candidate to investigate direct effects on neuronal function integrity and potential preventive effects on autoimmune neurodegeneration. Similarly to a recent study, BAF312 was applied either

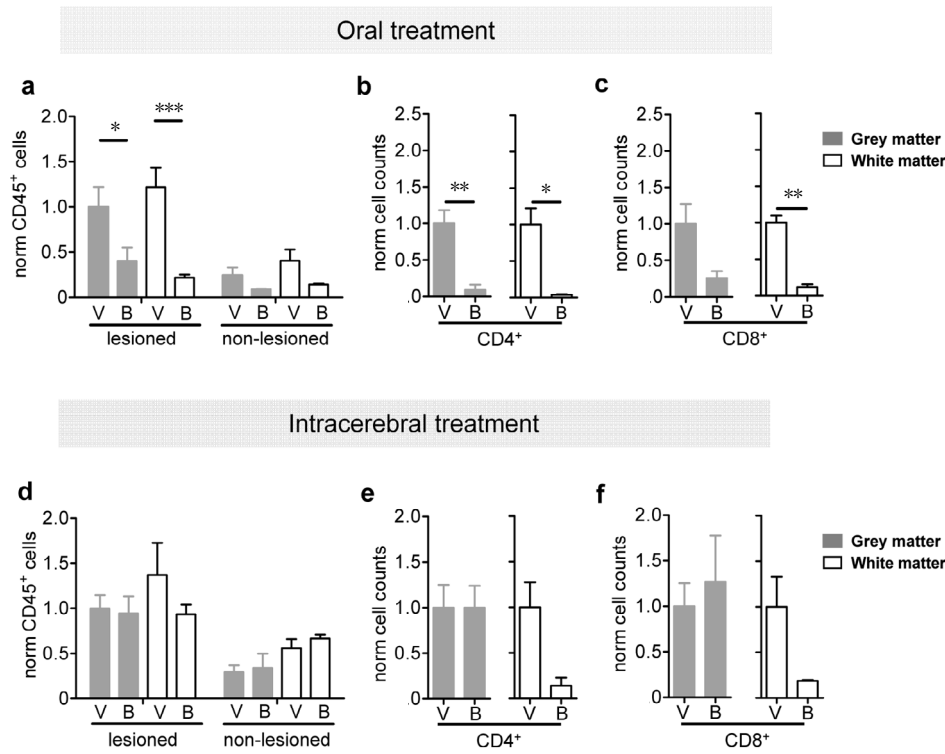


**Figure 2** Intracerebral treatment does not affect harmful immune cell infiltration into the brain parenchyma compared to non-treated controls.

(a) Bar graphs showing significant decrease of brain-infiltrating total CD45<sup>+</sup> leucocytes in the lesioned hemisphere after oral treatment with BAF312 (B; a novel sphingosine-1 receptor modulator) compared to vehicle-treated controls (V) both in grey (grey bars) and white matter (open bars). (b and c) Bar graphs showing significant decrease of CD4<sup>+</sup> (b) and CD8<sup>+</sup> lymphocytes (c) in the lesioned hemisphere after oral treatment with BAF312 (B) compared to vehicle-treated controls (V) both in grey (grey bars) and white matter (open bars). (d) Intracerebral treatment with BAF312 (B) did not affect the number of brain-infiltrating total CD45<sup>+</sup> leucocytes in both lesioned and non-lesioned hemispheres. No differences between grey (grey bars) and white matter (open bars) localization were observed. (e and f) Intracerebral treatment with BAF312 (B) did not affect the number of CD4<sup>+</sup> (E) and CD8<sup>+</sup> (F) lymphocytes in the lesioned hemisphere compared to vehicle-treated controls (V) both in grey (grey bars) and white matter (open bars). \**P* < 0.05, \*\**P* < 0.01, \*\*\**P* < 0.001 (two-way analysis of variance with Bonferroni *post-hoc* test for a and d and Student's *t*-test for the other analyses).

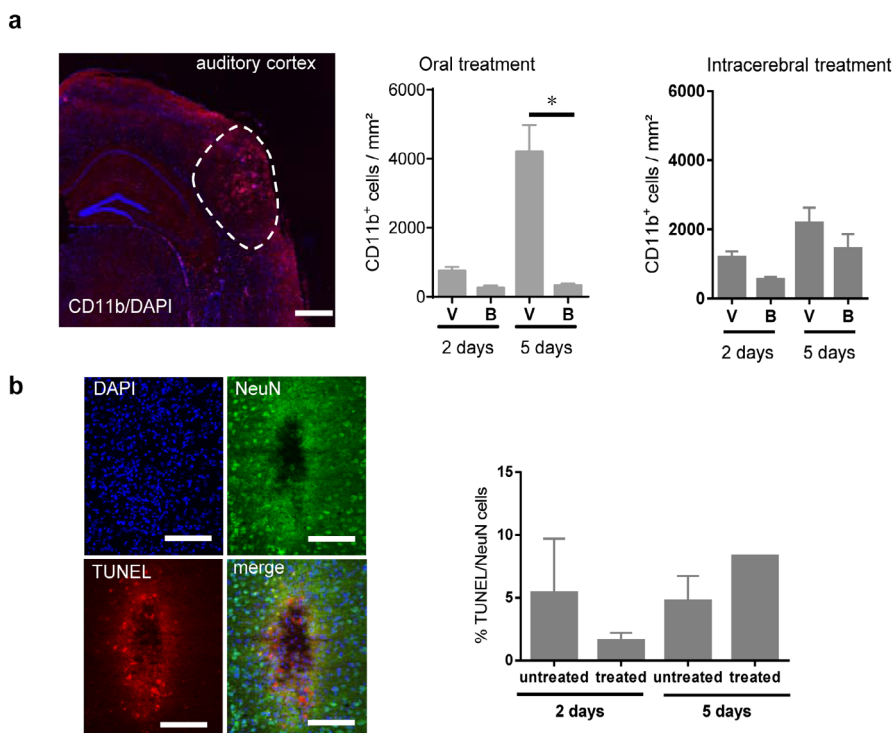


**Figure 3** Immunofluorescence staining show CD11b<sup>+</sup> cells infiltration in the focal lesions in the auditory cortex.

(a) Exemplary picture of a coronal brain slice containing the auditory cortex (delimited by the dashed area) showing the focal injection site. Infiltrating CD11b<sup>+</sup> cells are attracted to the injection site marked in red and cell nuclei in blue (DAPI). Bar graphs on the right side show quantification of CD11b<sup>+</sup> cells/mm<sup>2</sup> in vehicle (V) and BAF312 (a sphingosine-1-phosphate receptor modulator) treated mice for both oral and intracerebral treatment. Quantification was performed 2- and 5 days after focal cytokine injection. \**P* < 0.05 (Kruskal-Wallis test followed by Dunn's *post-hoc* test). Scale bar: 100 μm. (b) Representative images showing a high magnification of the focal injection site in the auditory cortex. Slices were stained for identification of cell nuclei (DAPI, blue), neuronal soma (NeuN, green) and the apoptotic marker TUNEL (red). On the right side of the panel, bar graphs showing the quantification of TUNEL/NeuN positive cells (cells/mm<sup>2</sup>) in vehicle (V) and BAF312 (B) treated mice for both oral and intracerebral administration. Quantification was performed 2- and 5 days after focal cytokine. Scale bars: 50 μm.

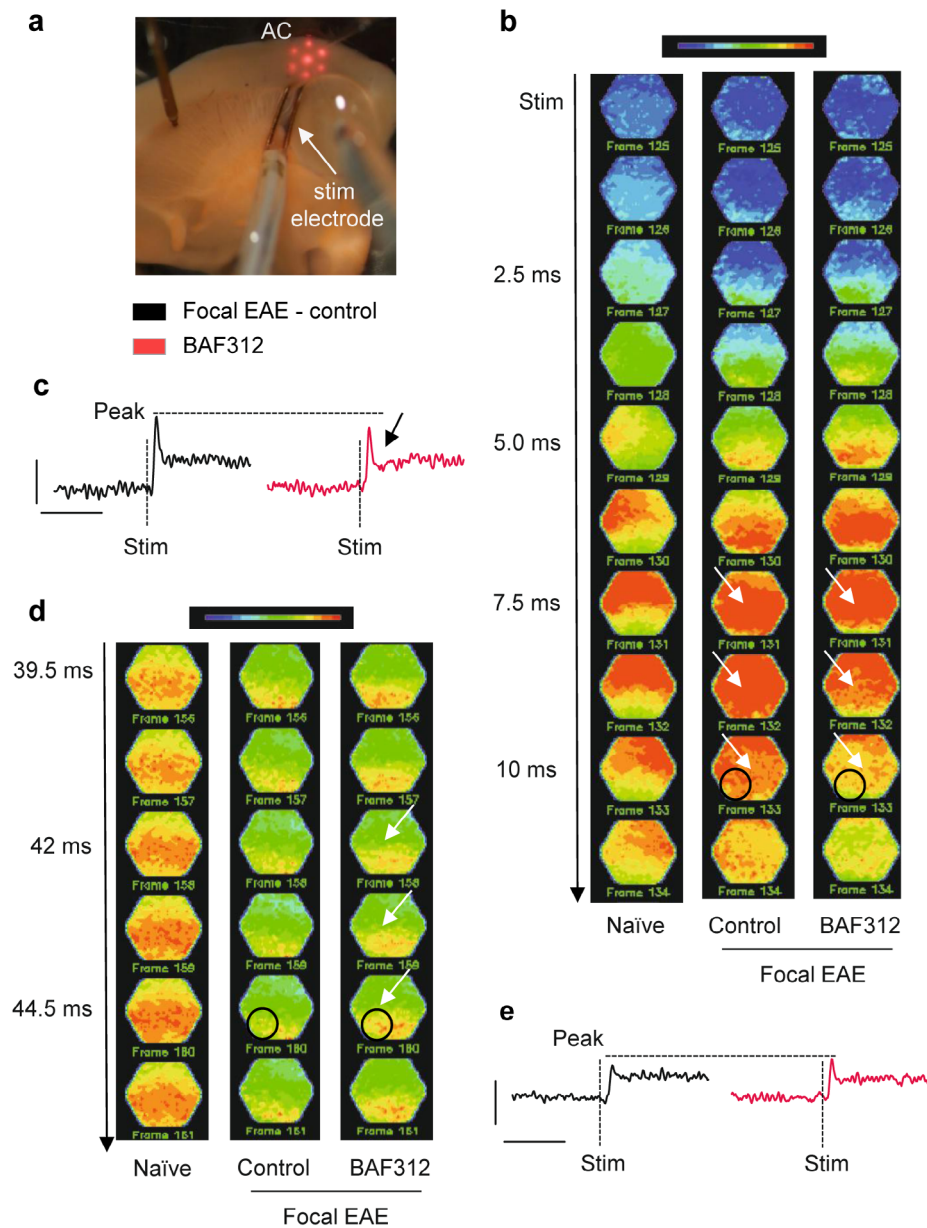


**Figure 4 Application of BAF312 to living brain slices restores changes in the spatio-temporal pattern of stimulus-induced propagation in the AC neuronal network.**

(a) Exemplary photo of a sagittal acute brain slice containing the AC and the internal capsule where the position of the stimulation electrode (stim electrode) is indicated by a white arrow. The hexagonal photodiode array used for the detection of the fractional changes of fluorescence signals is visible on the AC (red hexagonal structure). (b) Exemplary color-coded fluorescence maps of spatio-temporal patterns of activity in AC during the first ~13 seconds in response to electrical stimulation. The first map from the left represents neuronal activation of AC only in naïve animals that did not undergo general immunization or focal EAE induction. The upper layers of the AC corresponding to the upper parts of the maps respond firstly to an incoming stimulus and then information is further processed by propagating to the lower layers, as indicated by preponderance of warm colors in the lower part of the maps (scale: 0.34% dI/I). Maps obtained from animals with focal EAE (control in the text, second map from the left) show an abnormally high response to electrical stimulation indicated by the strong preponderance of warm colors filling the entire hexagonal structure as indicated by the white arrows (scale: 0.19% dI/I). After washing the slice for 30 minutes with a solution containing 10  $\mu$ M BAF312 (a sphingosine-1-phosphate receptor modulator), electrical stimulation evokes a slightly more articulated response in the cortex (third map from the left; scale: 0.15% dI/I). A spatio-temporal pattern of activation similar to control is observed upon BAF312 treatment as indicated by the white arrows. (c) Averaged exemplary fluorescence signals, recorded in the area contained in the black circle, showed a reduced amplitude by comparing control-peak vs. BAF312-treated peak of the response (horizontal dashed line). Moreover, following BAF312 treatment the repolarization phase after response is very steep, as indicated by the black arrow. (d) Exemplary color-coded fluorescence maps of spatio-temporal patterns of activity in AC between ~40 and 45 seconds after electrical stimulation showing propagation of the stimulus to lower layers of AC. The first map from the left represents AC neuronal activity in naïve animals that did not undergo general immunization or focal EAE induction. The second map from the left represents reduced stimulus propagation in animals with focal EAE (control). Application of BAF312 slightly increased the neuronal activity in the same part of the cortex, as indicated by the white arrows in the third map from the left. (e) Averaged exemplary fluorescence signal, recorded in the area contained in the black circle, between ~40 and 45 seconds after electrical stimulation shows a small increase in the amplitude of the propagated stimulus in BAF312-treated slices in comparison with control. Siponimod (BAF312): Novel sphingosine-1 receptor modulator; AC: auditory cortex; EAE: experimental autoimmune encephalomyelitis.

systemically or locally to the brain by using osmotic mini pumps (Gentile et al., 2016). In line with previous findings, systemic administration of BAF312 induced lymphopenia in our model (Choi et al., 2011; Gentile et al., 2016), while local treatment with continuous intracerebral administration had almost no effect on peripheral lymphocyte counts. Intuitively, this result is not surprising as only very confined brain regions were treated in mice which were already pre-immunized and that had a quite high number of activated immune cells. However, since one of our goal was to investigate potential contribution from different brain regions to the pathophysiology of the disease, as described already for MS both in patients and mice (De Stefano et al., 2003; Roosendaal et al., 2011; Narayanan et al., 2018), we assessed the number of cells within grey and white matter lesions. We found lower inflammatory cell infiltration in cortical grey matter lesions than in white matter lesions, as previously described (Peterson et al., 2001; Bø et al., 2003a). This condition was statistically unaffected by intracerebral BAF312 treatment although we did observe a tendency to CD4<sup>+</sup> and CD8<sup>+</sup> T cells reduction in the white matter only. In accordance to such small size effect, intracerebral treatment did not affect the clinical course in either group. In this respect, the experimental outline was designed to investigate brain therapeutic effects of BAF312 resembling intervention as similarly done in the majority of MS patients when diagnosed with new lesions as they are known to potentially trigger neuronal damage and loss. Because of our experimental settings, the treatment with BAF312 was relatively short, lasting only 2 days after injection of cytokines. Moreover, unlike previous studies (Gentile et al., 2016), here we investigated the effects of intracerebral administration of BAF312 only in those regions where inflammatory lesions were experimentally induced. However, white and grey matter lesions do randomly appear in the brain of EAE animals and where not investigated in this study.

Studying neuronal circuits in the context of autoimmune encephalitis has long been a challenge due to a lack of an appropriate lesion model and a convenient technique to ascertain differences in neuronal networks functioning. To take this challenge, we investigated the TC auditory pathway of our focal EAE mice by using voltage-sensitive dye imaging. The dye offers the possibility to visualize the local activity of large neuronal populations with high spatio-temporal resolution (Chemla and Chavane, 2010). In this study, we chose the AC as a very highly topographically organized grey matter region receiving inputs from subcortical regions *via* the IC (Barbour and Callaway, 2008). Here, we detected changes in AC neuronal network functionality in acute brain slices with cortical inflammatory lesions. In response to electrical stimulation, we observed altered overall neuronal activity. In line with recent evidence, the occurrence of demyelinating (Ghaffarian et al., 2016; Araújo et al., 2017; Cerina et al., 2017) or inflammatory lesions (Olechowski et al., 2013; Falco et al., 2014; Gentile et al., 2016; Potter et al., 2016) in grey matter profoundly affects neuronal excitability, our results would suggest a diminished ability of the cortical neuronal

network to properly distribute incoming information to the cortex (Broicher et al., 2010; Araújo et al., 2017). Interestingly enough, spatio-temporal propagation of the stimulus in the inflamed auditory cortical network seemed to be partially restored by local bath application of BAF312 in acute brain slices obtained from animals with inflammatory lesions, underlining its role in neuroprotection. Despite being applied only in an *ex vivo* preparation, its suggested role in regulating abnormal responses in the brain would be corroborated by previous evidence showing that intracerebroventricular administration of BAF312 affects the functionality of GABAergic neurons (Gentile et al., 2016), an effect described at single cell level that can now be observed in a broader neuronal network. However, it is important to mention that the optical signal recorded here is composed of multiple components, including glial cells and excitatory/inhibitory neurons (Chemla and Chavane, 2010). In this study, further mechanistic considerations could not be made, as without pharmacological modulation, distinguishing between neuronal populations contributing to the signals is indeed difficult. However, glial contributions could be ruled out due to the kinetics of the response, known to be slower compared to that of neurons (Broicher and Speckmann, 2012). Given previous studies (Gentile et al., 2016; O'Sullivan et al., 2016), identifying a misbalance between excitatory and inhibitory system functionality as the reason for altered neuronal activity seems to be likely. Moreover, the findings with BAF312 are also in line with previous studies showing the effects of the first generation sphingosine 1-phosphat receptor modulator, fingolimod (FTY720). As BAF312, fingolimod is known to functionally sequester lymphocytes presumably by interrupting the recirculation of autoreactive T- and B-lymphocytes to the CNS (Müllershausen et al., 2009). In the relapsing-remitting disease course, treatment with fingolimod leads to a significantly reduced values for annualized relapse rate, disability progression and MRI markers for disease progression such as new lesions and percentage loss of total brain volume (Kappos et al., 2010). Like BAF312, fingolimod binds its receptors on glial cells and neurons (Miron et al., 2008) exerting beneficial treatment effects due to direct neuronal interactions independently from peripheral lymphocytes. However, oral fingolimod treatment failed to slow disease progression in primary PMS (Lublin et al., 2016) and effects of second generation drugs have to be assessed.

## Conclusions

The present investigation indicates how an approach combining active and focal EAE, recently described also by other groups, could be used to reproduce hallmarks of PMS in rodents. Moreover, this experimental approach represents a suitable model to demonstrate the neuroprotective activity of BAF312 in combination with voltage sensitive dye imaging of cortical neuronal networks. Indeed, while local administration of BAF at the tested dose did not influence the functional readouts assessed by the EAE score, cortical function was affected. Our results encourage further investigation of the potential neuroprotective effects of BAF312.

**Acknowledgments:** The authors would like to thank Monika Wart, Jeanette Budde, Carina Butz, and Frank Kurth (Department of Neurology with Institute of Translational Neurology, Westfälische Wilhelms-Universität, Germany) for the excellent technical assistance. The authors would like to thank Dr. Nick Fulcher (Department of Neurology with Institute of Translational Neurology, Westfälische Wilhelms-Universität, Germany) for proof-reading and editing the final version of the manuscript and to acknowledge the Graduate School of the Cells-in-Motion Cluster of Excellence (EXC 1003 – CiM) from the University of Münster, Germany.

**Author contributions:** PH designed, performed and analyzed the experiments, and supervised the project. PH, CT and MC wrote the manuscript. MC performed and analyzed voltage-sensitive dye imaging experiments together with EJS. CT, AMH, SE, TM and JFO helped in preparing the tissues for *ex vivo* evaluations. KG designed and performed the initial experiments. SE, SB and TR performed and analyzed the flow cytometry assays. VN performed the focal cytokine injections. AS provided the BAF312 on behalf of Novartis, participated in discussing results and proof-reading the manuscript. TB and EJS participated in discussing the data. HW and SGM designed and supervised the project. All authors approved the final version of the manuscript.

**Conflicts of interest:** SGM has received honoraria for lecturing, travel expenses for attending meetings and financial research support from Almirall, Bayer Health Care, Biogen, Celgene, Diamed, Fresenius Medical Care, Genzyme, Merck Serono, Novartis, Novo Nordisk, ONO Pharma, Roche, Sanofi-Aventis and Teva. HW has received honoraria for lecturing, travel expenses for attending meetings and financial research support from Alexion, Biogen, Cognomed, F. Hoffmann-La Roche Ltd., Gemeinnützige Hertie-Stiftung, Merck Serono, Novartis, Roche Pharma AG, Sanofi-Genzyme, TEVA, WebMD Global, Abbvie, Actelion, IGES, Novartis, Roche, Swiss Multiple Sclerosis Society. PH received honoraria for lecturing, travel expenses for attending meetings and financial research support from Novartis. MC received honoraria for lecturing, travel expenses for attending meetings and financial research support from Novartis. AS is a full-term employee of Novartis. TR received research support from Novartis and Sanofi Genzyme and honoraria for lecturing and travel expenses for attending meetings from Sanofi Genzyme, Novartis, TEVA, Biogen, Merck Serono and Roche. TB received financial research support from Biogen. The other co-authors declare no conflicts of interest.

**Financial support:** This study was supported by the Novartis Institutes of Biomedical Research, Basel, Switzerland (to SGM).

**Institutional review board statement:** Experiments were carried out in accordance with German and EU animal protection law and approved by local authorities (Landesamt für Natur, Umwelt und Verbraucherschutz Nordrhein-Westfalen; 87-51.04.2010.A331) on December 28, 2010.

**Copyright license agreement:** The Copyright License Agreement has been signed by all authors before publication.

**Data sharing statement:** Datasets analyzed during the current study are available from the corresponding author on reasonable request.

**Plagiarism check:** Checked twice by iThenticate.

**Peer review:** Externally peer reviewed.

**Open access statement:** This is an open access journal, and articles are distributed under the terms of the Creative Commons Attribution-NonCommercial-ShareAlike 4.0 License, which allows others to remix, tweak, and build upon the work non-commercially, as long as appropriate credit is given and the new creations are licensed under the identical terms.

**Open peer reviewer:** Wensheng Lin, University of Minnesota Twin Cities, USA.

**Additional files:**

**Additional Figure 1:** Central BAF application does not induce peripheral lymphopenia.

**Additional file 1:** Open peer review report 1.

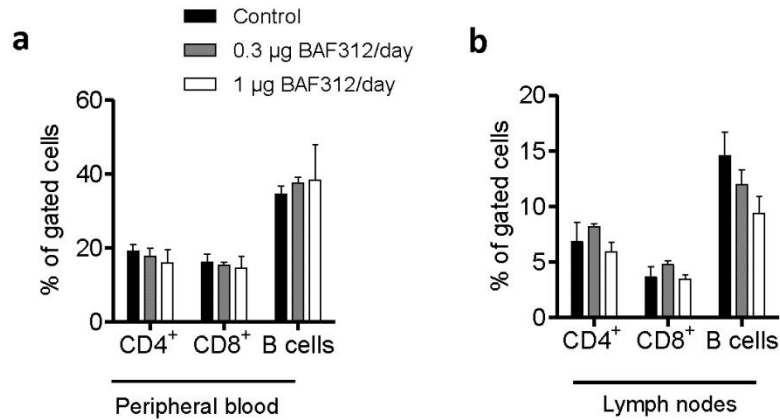
## References

Araújo SES, Mendonça HR, Wheeler NA, Campello-Costa P, Jacobs KM, Gomes FCA, Fox MA, Fuss B (2017) Inflammatory demyelination alters subcortical visual circuits. *J Neuroinflammation* 14:162.  
Barbour DL, Callaway EM (2008) Excitatory local connections of superficial neurons in rat auditory cortex. *J Neurosci* 28:11174-11185.  
Bigaud M, Guerini D, Billich A, Bassilana F, Brinkmann V (2014) Second generation S1P pathway modulators: Research strategies and clinical developments. *Biochim Biophys Acta* 1841:745-758.

Bittner S, Afzali AM, Wiendl H, Meuth SG (2014) Myelin oligodendrocyte glycoprotein (MOG35-55) induced experimental autoimmune encephalomyelitis (EAE) in C57BL/6 mice. *J Vis Exp* doi: 10.3791/51275.  
Bø L, Vedeler CA, Nyland H, Trapp BD, Mørk SJ (2003a) Intracortical multiple sclerosis lesions are not associated with increased lymphocyte infiltration. *Mult Scler* 9:323-331.  
Bø L, Vedeler CA, Nyland HI, Trapp BD, Mørk SJ (2003b) Subpial demyelination in the cerebral cortex of multiple sclerosis patients. *J Neuropathol Exp Neurol* 62:723-732.  
Broicher T, Bidmon H-J, Kamuf B, Coulon P, Gorji A, Pape HC, Speckmann EJ, Budde T (2010) Thalamic afferent activation of supragranular layers in auditory cortex in vitro: a voltage sensitive dye study. *Neuroscience* 165:371-385.  
Broicher T, Speckmann EJ (2012) Living Human Slices: Network Analysis Using Voltage Sensitive Dyes. In: Isolated Central Nervous System Circuits (Allany K, ed), pp 285-300. Totowa, NJ: Humana Press, Springer.  
Cerina M, Narayanan V, Göbel K, Bittner S, Ruck T, Meuth P, Herrmann AM, Stangel M, Gudi V, Skripuletz T, Daldrup T, Wiendl H, Seidenbecher T, Ehling P, Kleinschnitz C, Pape HC, Budde T, Meuth SG (2017) The quality of cortical network function recovery depends on localization and degree of axonal demyelination. *Brain Behav Immun* 59:103-117.  
Chaudhary P, Marracci G, Galipeau D, Pocius E, Morris B, Bourdette D (2015) Lipoic acid reduces inflammation in a mouse focal cortical experimental autoimmune encephalomyelitis model. *J Neuroimmunol* 289:68-74.  
Chemla S, Chavane F (2010) Voltage-sensitive dye imaging: Technique review and models. *J Physiol Paris* 104:40-50.  
Choi JW, Gardell SE, Herr DR, Rivera R, Lee C-W, Noguchi K, Teo ST, Yung YC, Lu M, Kennedy G, Chun J (2011) FTY720 (fingolimod) efficacy in an animal model of multiple sclerosis requires astrocyte sphingosine 1-phosphate receptor 1 (S1P1) modulation. *Proc Natl Acad Sci U S A* 108:751-756.  
De Stefano N, Matthews PM, Filippi M, Agosta F, De Luca M, Bartolozzi ML, Guidi L, Ghezzi A, Montanari E, Cifelli A, Federico A, Smith SM (2003) Evidence of early cortical atrophy in MS: Relevance to white matter changes and disability. *Neurology* 60:1157-1162.  
Deppe M, Krämer J, Tenberge JG, Marinell J, Schwindt W, Deppe K, Groppa S, Wiendl H, Meuth SG (2016) Early silent microstructural degeneration and atrophy of the thalamocortical network in multiple sclerosis. *Hum Brain Mapp* 37:1866-1879.  
Falco A, Pennucci R, Brambilla E, de Curtis I (2014) Reduction in parvalbumin-positive interneurons and inhibitory input in the cortex of mice with experimental autoimmune encephalomyelitis. *Exp Brain Res* 232:2439-2449.  
Frischer JM, Weigand SD, Guo Y, Kale N, Parisi JE, Pirko I, Mandrekar J, Bramow S, Metz I, Brück W, Lassmann H, Lucchinetti CF (2015) Clinical and pathological insights into the dynamic nature of the white matter multiple sclerosis plaque. *Ann Neurol* 78:710-721.  
Gentile A, Musella A, Bullitta S, Fresegna D, De Vito F, Fantozzi R, Piras E, Gargano F, Borsellino G, Battistini L, Schubart A, Mandolesi G, Centonze D (2016) Siponimod (BAF312) prevents synaptic neurodegeneration in experimental multiple sclerosis. *J Neuroinflammation* 13:207.  
Gergely P, Nuesslein-Hildesheim B, Guerini D, Brinkmann V, Traebert M, Bruns C, Pan S, Gray NS, Hinterding K, Cooke NG, Groenewegen A, Vitaliti A, Sing T, Luttringer O, Yang J, Gardin A, Wang N, Crumb WJ Jr, Saltzman M, Rosenberg M, et al. (2012) The selective sphingosine 1-phosphate receptor modulator BAF312 redirects lymphocyte distribution and has species-specific effects on heart rate. *Br J Pharmacol* 167:1035-1047.  
Ghaffarian N, Mesgari M, Cerina M, Göbel K, Budde T, Speckmann EJ, Meuth SG, Gorji A (2016) Thalamocortical-auditory network alterations following cuprizone-induced demyelination. *J Neuroinflammation* 13:160.  
Göbel K, Pankratz S, Asaridou CM, Herrmann AM, Bittner S, Merker M, Ruck T, Glumm S, Langhauser F, Kraft P, Krug TF, Breuer J, Herold M, Gross CC, Beckmann D, Korb-Pap A, Schuhmann MK, Kuerten S, Mitroulis I, Ruppert C, et al. (2016a) Blood coagulation factor XII drives adaptive immunity during neuroinflammation via CD87-mediated modulation of dendritic cells. *Silent Commun* 7:11626.

- Göbel K, Kraft P, Pankratz S, Gross CC, Korsukewitz C, Kwicien R, Mesters R, Kehrel BE, Wiendl H, Kleinschnitz C, Meuth SG (2016b) Prothrombin and factor X are elevated in multiple sclerosis patients. *Ann Neurol* 80:946-951.
- Haider L, Simeonidou C, Steinberger G, Hametner S, Grigoriadis N, Deretzi G, Kovacs GG, Kutzelnigg A, Lassmann H, Frischer JM (2014) Multiple sclerosis deep grey matter: the relation between demyelination, neurodegeneration, inflammation and iron. *J Neurol Neurosurg Psychiatry* 85:1386-1395.
- Jaillard C, Harrison S, Stankoff B, Aigrot MS, Calver AR, Duddy G, Walsh FS, Pangalos MN, Arimura N, Kaibuchi K, Zalc B, Lubetzki C (2005) Edg8/S1P5: an oligodendroglial receptor with dual function on process retraction and cell survival. *J Neurosci* 25:1459-1469.
- Johns TG, Kerlero de Rosbo N, Menon KK, Abo S, Gonzales MF, Bernard CC (1995) Myelin oligodendrocyte glycoprotein induces a demyelinating encephalomyelitis resembling multiple sclerosis. *J Immunol* 154:5536-5541.
- Kappos L, Bar-Or A, Cree BAC, Fox RJ, Giovannoni G, Gold R, Vermersch P, Arnold DL, Arnould S, Scherz T, Wolf C, Wallström E, Dahlke F; EXPAND Clinical Investigators (2018) Siponimod versus placebo in secondary progressive multiple sclerosis (EXPAND): a double-blind, randomised, phase 3 study. *Lancet* 391:1263-1273.
- Kappos L, Radue E-W, O'Connor P, Polman C, Hohlfeld R, Calabresi P, Selmaj K, Agoropoulou C, Leyk M, Zhang-Auberson L, Burtin P (2010) A Placebo-Controlled Trial of Oral Fingolimod in Relapsing Multiple Sclerosis. *N Engl J Med* 362:387-401.
- Kerschensteiner M, Stadelmann C, Buddeberg BS, Merkler D, Bareyre FM, Anthony DC, Linington C, Brück W, Schwab ME (2004) Targeting experimental autoimmune encephalomyelitis lesions to a pre-determined axonal tract system allows for refined behavioral testing in an animal model of multiple sclerosis. *Am J Pathol* 164:1455-1469.
- Kidd D, Barkhof F, McConnell R, Algra PR, Allen IV, Revesz T (1999) Cortical lesions in multiple sclerosis. *Brain* 122:17-26.
- Klotz L, Havla J, Schwab N, Hohlfeld R, Barnett M, Reddel S, Wiendl H (2019) Risks and risk management in modern multiple sclerosis immunotherapeutic treatment. *Ther Adv Neurol Disord* 12:1756286419836571.
- Kuhlmann T, Ludwin S, Prat A, Antel J, Brück W, Lassmann H (2017) An updated histological classification system for multiple sclerosis lesions. *Acta Neuropathol* 133:13-24.
- Lagumersindez-Denis N, Wrzoc C, Mack M, Winkler A, van der Meer F, Reinert MC, Hollasch H, Flach A, Brühl H, Cullen E, Schlumbohm C, Fuchs E, Linington C, Barrantes-Freer A, Metz I, Wegner C, Liebetanz D, Prinz M, Brück W, Stadelmann C, et al. (2017) Differential contribution of immune effector mechanisms to cortical demyelination in multiple sclerosis. *Acta Neuropathol* 134:15-34.
- Lassmann H, Bradl M (2016) Multiple sclerosis: experimental models and reality. *Acta Neuropathol* 133:1-22.
- Lublin F, Miller DH, Freedman MS, Cree BAC, Wolinsky JS, Weiner H, Lubetzki C, Hartung HP, Montalban X, Uitdehaag BMJ, Merschhemke M, Li B, Putzki N, Liu FC, Häring DA, Kappos L; INFORMS study investigators (2016) Oral fingolimod in primary progressive multiple sclerosis (INFORMS): A phase 3, randomised, double-blind, placebo-controlled trial. *Lancet* 387:1075-1084.
- Lublin FD, Reingold SC, Cohen JA, Cutter GR, Sørensen PS, Thompson AJ, Wolinsky JS, Balcer LJ, Banwell B, Barkhof F, Bebo B Jr, Calabresi PA, Clanet M, Comi G, Fox RJ, Freedman MS, Goodman AD, Inglesse M, Kappos L, Kieseier BC, et al. (2014) Defining the clinical course of multiple sclerosis: The 2013 revisions. *Neurology* 83:278-286.
- Mandolesi G (2015) Synaptopathy connects inflammation and neurodegeneration in multiple sclerosis. *Nat Rev Neurol* 11:711-724.
- Mendel I, de Rosbo NK, Ben-Nun A (1995) A myelin oligodendrocyte glycoprotein peptide induces typical chronic experimental autoimmune encephalomyelitis in H-2b mice: Fine specificity and T cell receptor Vbeta expression of encephalitogenic T cells. *Eur J Immunol* 25:1951-1959.
- Merkler D, Ernsting T, Kerschensteiner M, Brück W, Stadelmann C (2006) A new focal EAE model of cortical demyelination: multiple sclerosis-like lesions with rapid resolution of inflammation and extensive remyelination. *Brain* 129:1972-1983.
- Miron VE, Schubart A, Antel JP (2008) Central nervous system-directed effects of FTY720 (fingolimod). *J Neurol Sci* 274:13-17.
- Montalban X, Hauser SL, Kappos L, Arnold DL, Bar-Or A, Comi G, de Seze J, Giovannoni G, Hartung HP, Hemmer B, Lublin F, Rammohan KW, Selmaj K, Traboulsee A, Sauter A, Masterman D, Fontoura P, Belachew S, Garren H, Mairon N, et al. (2017) Ocrelizumab versus Placebo in Primary Progressive Multiple Sclerosis. *N Engl J Med* 376:209-220.
- Mullershausen F, Zecri F, Cetin C, Billich A, Guerini D, Seuwen K (2009) Persistent signaling induced by FTY720-phosphate is mediated by internalized S1P1 receptors. *Nat Chem Biol* 5:428-434.
- Narayanan V, Cerina M, Göbel K, Meuth P, Herrmann AM, Fernandez-Orth J, Stangel M, Gudi V, Skripuletz T, Daldrop T, Lesting J, Schiffler P, Wiendl H, Seidenbecher T, Meuth SG, Budde T, Pape H-C (2018) Impairment of frequency-specific responses associated with altered electrical activity patterns in auditory thalamus following focal and general demyelination. *Exp Neurol* 309:54-66.
- O'Sullivan C, Schubart A, Mir AK, Dev KK (2016) The dual S1PR1/S1PR5 drug BAF312 (Siponimod) attenuates demyelination in organotypic slice cultures. *J Neuroinflammation* 13:31.
- Olechowski CJ, Tenorio G, Sauve Y, Kerr BJ (2013) Changes in nociceptive sensitivity and object recognition in experimental autoimmune encephalomyelitis (EAE). *Exp Neurol* 241:113-121.
- Pan S, Gray NS, Gao W, Mi Y, Fan Y, Wang X, Tuntland T, Che J, Lefebvre S, Chen Y, Chu A, Hinterding K, Gardin A, End P, Heining P, Bruns C, Cooke NG, Nuesslein-Hildesheim B (2013) Discovery of BAF312 (Siponimod), a potent and selective S1P receptor modulator. *ACS Med Chem Lett* 4:333-337.
- Paxinos G, Franklin KBJ (2001) The mouse brain in stereotaxic coordinates, 2nd ed. San Diego: Academic Press.
- Peterson JW, Bö L, Mörk S, Chang A, Trapp BD (2001) Transected neurites, apoptotic neurons, and reduced inflammation in cortical multiple sclerosis lesions. *Ann Neurol* 50:389-400.
- Pomeroy IM, Matthews PM, Frank JA, Jordan EK, Esiri MM (2005) Demyelinated neocortical lesions in marmoset autoimmune encephalomyelitis mimic those in multiple sclerosis. *Brain* 128:2713-2721.
- Potter LE, Paylor JW, Suh JS, Tenorio G, Caliaperumal J, Colbourne F, Baker G, Winship I, Kerr BJ (2016) Altered excitatory-inhibitory balance within somatosensory cortex is associated with enhanced plasticity and pain sensitivity in a mouse model of multiple sclerosis. *J Neuroinflammation* 13:142.
- Roosendaal SD, Bendfeldt K, Vrenken H, Polman CH, Borgwardt S, Radue EW, Kappos L, Pelletier D, Hauser SL, Matthews PM, Barkhof F, Geurts JJ (2011) Grey matter volume in a large cohort of MS patients: relation to MRI parameters and disability. *Mult Scler J* 17:1098-1106.
- Schneider CA, Rasband WS, Eliceiri KW (2012) NIH Image to ImageJ: 25 years of image analysis. *Nat Methods* 9:671-675.
- Silva BA, Leal MC, Farias MI, Avalos JC, Besada CH, Pitossi FJ, Ferrari CC (2018) A new focal model resembling features of cortical pathology of the progressive forms of multiple sclerosis: Influence of innate immunity. *Brain Behav Immun* 69:515-531.
- Simmons RD, Willenborg DO (1990) Direct injection of cytokines into the spinal cord causes autoimmune encephalomyelitis-like inflammation. *J Neurol Sci* 100:37-42.
- Storch MK, Bauer J, Linington C, Olsson T, Weissert R, Lassmann H (2006) Cortical demyelination can be modeled in specific rat models of autoimmune encephalomyelitis and is major histocompatibility complex (MHC) haplotype-related. *J Neuropathol Exp Neurol* 65:1137-1142.
- Sun D, Newman TA, Perry VH, Weller RO (2004) Cytokine-induced enhancement of autoimmune inflammation in the brain and spinal cord: Implications for multiple sclerosis. *Neuropathol Appl Neurobiol* 30:374-384.
- Toader LE, Rosu GC, Catalin B, Tudorica V, Pirici I, Taisescu O, Muresanu DF (2018) Clinical and histopathological assessment on an animal model with experimental autoimmune encephalomyelitis. *Curr Heal Sci J* 44:280-287.

P-Reviewer: Lin W; C-Editors: Zhao M, Li CH; T-Editor: Jia Y



**Additional Figure 1 Central BAF application does not induce peripheral lymphopenia.**

(a) Bar graph showing the percentage of peripheral blood lymphocytes in animals with focal EAE, two days after pump implantation and intracerebral injections of a solution containing either vehicle, BAF312 0.3 µg/day or BAF312 1 µg/day. No differences can be observed when the two different doses are compared. (b) Bar graph showing the percentage of isolated lymphocytes in animals with focal EAE, two days after pump implantation and intracerebral injections of a solution containing either vehicle, BAF312 0.3 µg/day or BAF312 1 µg/day. No differences can be observed when the two different doses are compared.